Supplementary Materials for

A novel peptide protects against diet-induced obesity by suppressing appetite and modulating the gut microbiota

Methods

Cytotoxicity of D3

A Cell Titer Glo kit was used to measure the cytotoxicity of D3 on the viability of HCT116 cells according to the manufacturer's instructions. Briefly, HCT116 cells were seeded into a 384-well cell plate (1000 cells/well) and incubated overnight at 37 °C and 5% (v/v) CO_2. D3 at different concentrations was coincubated with cells for another 72 h at 37 °C and 5% (v/v) CO_2. Finally, the luminescence signal was recorded by an Envision microplate reader.

The hemolytic activity of D3 was evaluated by determining the amount of hemoglobin released from the blood cells. Mouse erythrocytes were collected and washed three times with PBS (pH 7.2) and then centrifuged at 1,500 rpm for 10 min. Then, 100 μl of erythrocyte solution (8%, v/v) was mixed with 100 μl of a series of peptide solutions and incubated for 1 h at 37 °C. The mixture was then centrifuged at 1,500 rpm for 5 min, and the absorbance of supernatants was measured at 540 nm. Values of 0 and 100% hemolysis were determined in PBS and 0.1% Triton X-100, respectively. Three replicates were performed for each condition. Hemolysis (%) = [Abs540 nm of the treated sample - Abs540 nm of the negative control)/(Abs540 nm of the positive control - Abs540 nm of the negative control)] × 100.

Leptin sensitivity measurement

The first assay is to determine the responses of body weight to leptin administration, which was performed according to the procedure proposed by Yu et al.[1, 2]. After 10 weeks of HFD or D3 treatment, the mice in each group were divided into two subgroups and received intraperitoneally administered leptin (1 μg/g body weight) or vehicle twice daily for 3 days. Recombinant murine leptin (ChinaPeptides Co., Ltd.) was dissolved in 0.9% NaCl solution and sterile filtered through a 0.22-μm

Li Z, *et al. Gut* 2022;0:1–13. doi: 10.1136/gutjnl-2022-328035

filter. Body weights were measured twice daily before and after the leptin injection.

The second assay is to detect the leptin-stimulated cytokines according to previous studies[3, 4]. After 8 weeks of HFD or D3 treatment, Mice were injected ip with leptin (5.0 mg/kg body weight) or vehicle (PBS) and anesthetized 25 min later, and the brains were immediately removed, frozen and stored at −80 °C. The mRNA of SOCS-3, PTP1B and PI3K was quantified by RT-PCR using RNA isolated from microdissected arcuate nucleus[5].

Indirect calorimetry

The metabolic parameters oxygen consumption (VO2) and carbon dioxide production (VCO2) were determined by an indirect calorimetry system (TSE Systems, Bad Homburg, Germany)[6]. Briefly, mice were acclimated in training cages for 3 days prior to the measurement and were allowed 4 additional days to acclimate to the TSE cabinets92. Gas exchanges were recorded every 20 minutes over 20 hours.

Glucose tolerance testing

After fasting for 6 h, mice were treated with oral gavage glucose (2 g/kg body weight)[7, 8] at 9:00 a.m. Blood samples were collected from the tip of the tail vein, and blood glucose was measured at 0 (immediately before glucose injection), 15, 30, 60 and 120 min with a Freestyle Lite glucose meter (Accu Check, Roche, Switzerland).

Insulin tolerance test (ITT)

Mice were intraperitoneally injected with insulin (1.0 U/kg body weight) at 9:00 a.m. Blood glucose levels were measured from the tail vein at 0, 15, 30, 60, 90, and 120 min as described above[7, 8].

DNA isolation, 16S rRNA sequencing and quantitative PCR

Bacterial DNA was extracted from the fecal samples using a QIAamp-DNA mini stool kit (QIAGEN, CA, USA). After 16S rRNA (V3-V4) amplicon sequencing, the abundance and diversity of intestinal flora in mice were determined using Illumina HiSeq sequencing (I-Sanger, Beijing, China). The QIIME software package was used to conduct the bioinformatic analyses of the sequences as described previously. Sequences with 97% sequence identity were attributed to the same operational taxonomic units (OTUs), and the OTU table was picked using the open reference

picking strategy based on the Greengenes database. Linear discriminant analysis (LDA) effect size (LEfSe) analysis was conducted to identify discriminatory bacteria, with an absolute value of the log LDA score >3.0 being considered a differential signature, which was significantly better in discriminating between different groups. QIME was used for principal coordinate analysis depending on the unweighted UniFrac distances, and intergroup comparisons were conducted using Wilcoxon rank-sum tests.

A. muciniphila was quantified with qPCR as described in Everard et al.[9]. Briefly, a total of 10 ng of DNA was used for quantitative PCR (qPCR). Primers for *A. muciniphila* (AM1: 5'-CAGCACGTGAAGGTGGGGAC-3', AM2: 5'-CCTTGCGGTTGGCTTCAGAT-3') and total bacteria (27F: 5'-AGAGTTTGATCCTGGCTCAG-3', 1492R: 5'-GGWTACCTTGTTACGACTT-3') and the relative abundance of target bacteria were calculated using the $2^{-\Delta\Delta Ct}$ method.

RNA extraction, and RT-qPCR, and RNA-seq data analysis

Total RNA was extracted from the ileum or fat tissue of animals using TRIzol reagent (Invitrogen, Carlsbad, CA) according to the manufacturer's instructions. cDNA was prepared by reverse transcription of 1-2 μg total RNA with reverse transcription enzyme (Yeasen, Shanghai, China). The target primers used are listed in Supplementary Table 2. qPCR detection was performed with the StepOnePlus real-time PCR system and software (Applied Biosystems, Foster City, USA). The results of gene expression are presented as a percentage expression of each gene normalized with glyceraldehyde-3-phosphate dehydrogenase (GAPDH) as a reference. RNA-seq data were first trimmed to remove low-quality bases using trim galore v0.4.4. HISAT2 v2.0.5 and StringTie v1.3.4[10] were used to quantify gene abundance with GRCm38 as the mouse reference genome. Differential expression (DE) analysis was performed using DESeq2 v1.24.0. Genes with significant DE were those with a 2-fold change cutoff and an adjusted P value < 0.05. Gene Ontology enrichment analysis (GOEA) was performed using the R package cluster Profiler v3.12.0. The results of GOEA were visualized in Goplot v1.0.2[11].

Supplementary figures

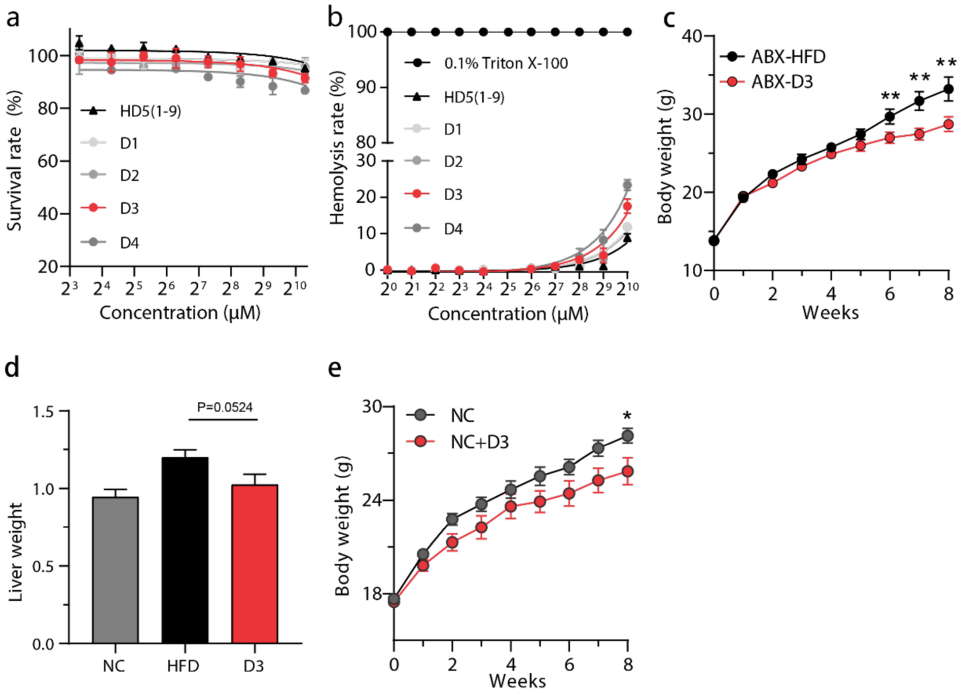

Supplementary Figure 1. Oral administration of D3 counteracts obesity. a, The cytotoxic activity of D1-4 to mouse Hct116 cells. The y-axis represents survival rate. **b**, Hemolytic activity of D1-4 against murine erythrocytes. **c**. Grams of weight gain measured over time, starting at 4 weeks of age (ABX: antibiotic mixture; n=6 per group). **d**, Total weight of liver. **e**. Grams of weight gain measured over time, starting at 4 weeks of age; (n=6 per group). For **a** and **b**, Deming regression was used to evaluate the trend in toxicity with different D3 concentrations. For **c-e**, *P* values were determined by a two-tailed Wilcoxon test, and data are presented as the means ± s.e.m; $P < 0.05$ (*); $P < 0.01$ (**).

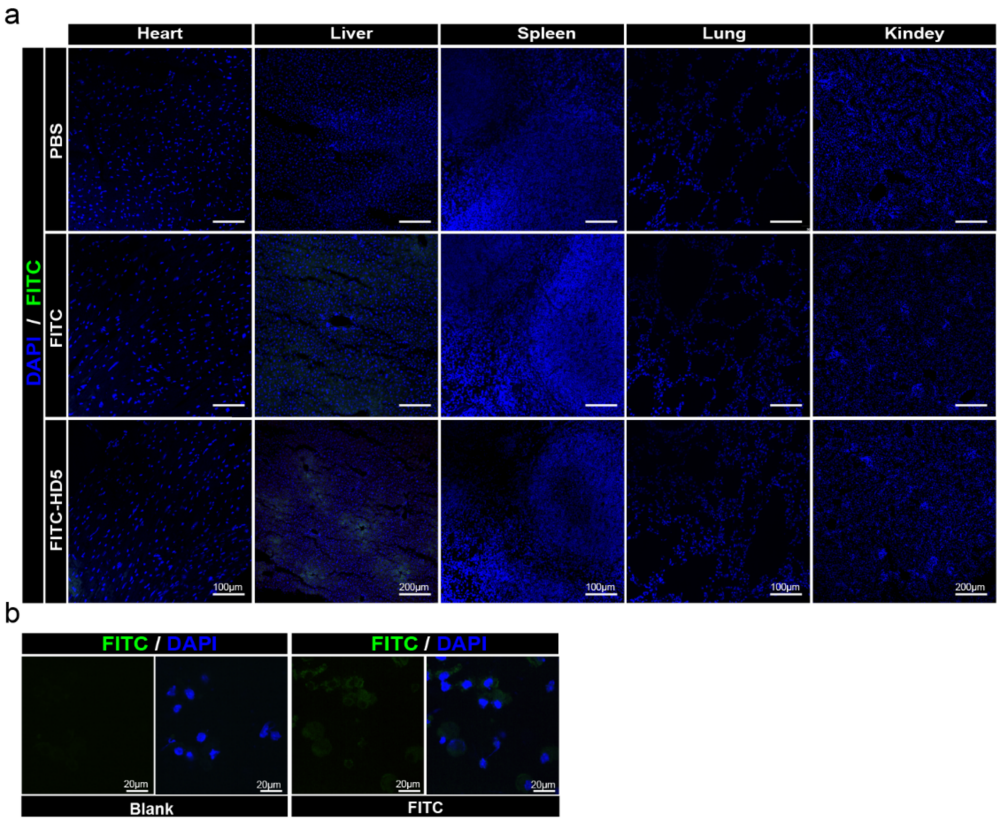

Supplementary Figure 2. Pharmacological distribution of FITC-D3 in other major viscera. a, Confocal images of sections from heart, liver, spleen, lung and kidney of SPF mice, three hours after oral administration of D3. Scale bars: 100/200 μm. **b**, Localization of FITC or FITC-D3 visualized by confocal microscopy. HCT 166 cells were incubated with 10 μM FITC and FITC-D3 (green) for 2 hours. Scale bars: 20 μm. Images are representative of three independent experiments with similar results.

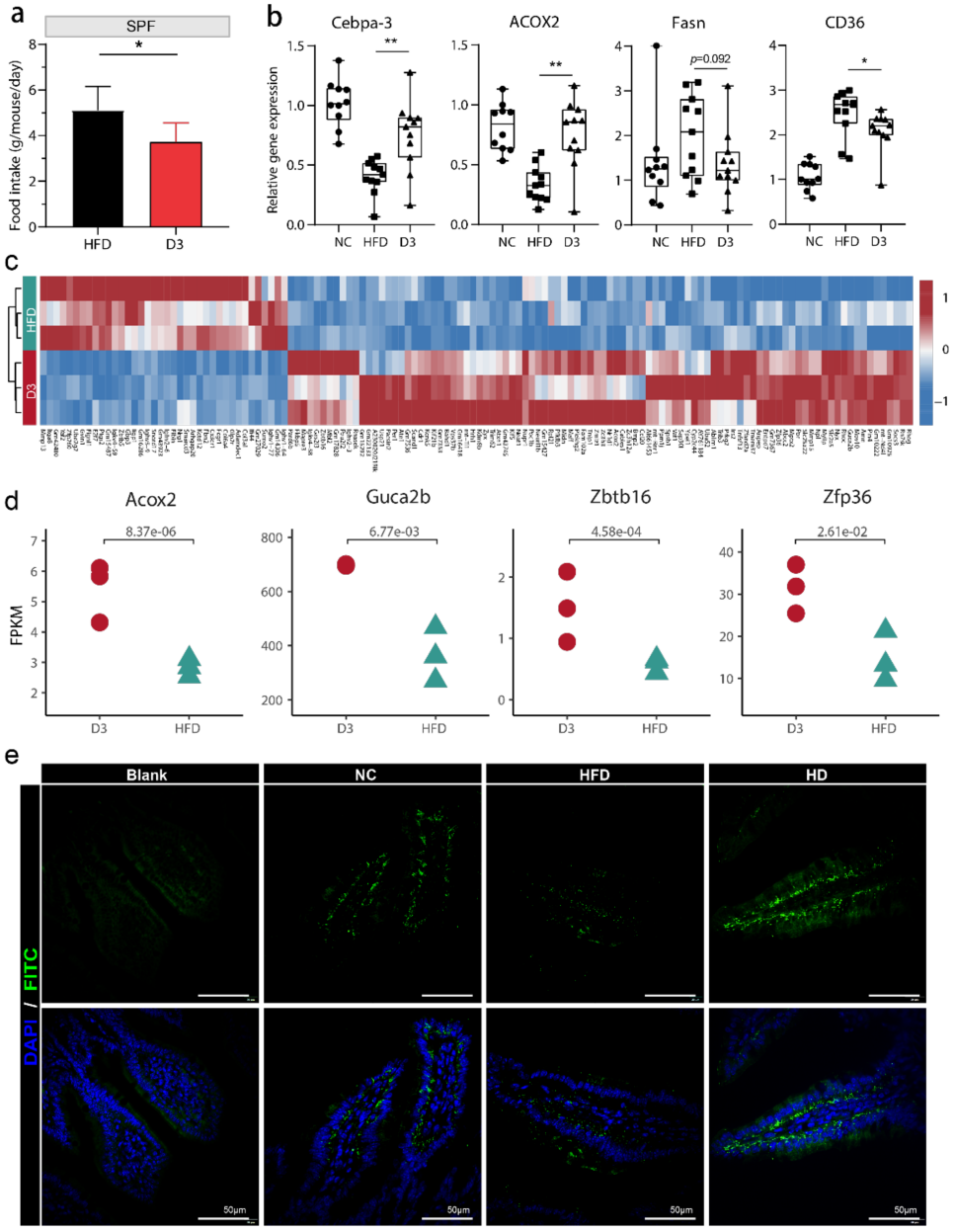

Supplementary Figure 3. Differentially expressed genes and immunofluorescence of UGN in ileum. a, Effect of D3 treatment on acute food intake, which was measured every other day for one week (SPF mice, n=10-12). **b**, Cebpa-3, Acox2, CD36 and Fasn (epididymis) mRNA expression levels of mice fed a control diet (NC and HFD) or treated with D3 (SPF mice, n=10-12). For **a** and **b**, *P* values were determined by a two-tailed Wilcoxon test, and data are presented as the means ± s.e.m; $P < 0.05$ (*); $P < 0.01$ (**). **c**, Clustering differentially expressed (DE) genes between HFD and D3. Different rows represent different samples and different columns represent DE genes. Relative levels of gene expression are depicted with a color scale in which red represents the highest level of up-regulated expression and blue represents the lowest level of down-

regulated expression. **d**, The relative expression levels of Acox2, Guca2b, Zfp36 and Zbtb16. P values were determined by two-tailed Wilcoxon test**. e**, Higher multiples of immunofluorescence in ileum sections for UGN (UGN, green) and nuclei (blue), while the diffuse green thin layer is a noisy background. Scale bars, 50 μm. Images are representative of three independent experiments with similar results.

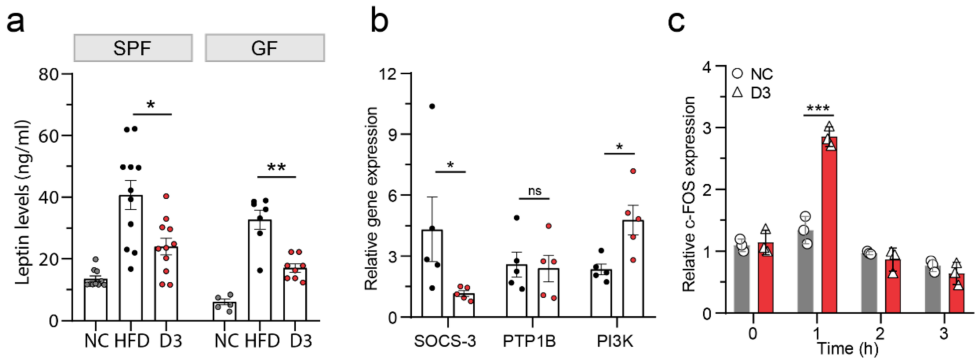

Supplementary Figure 4. D3 increases leptin sensitivity in mice. a, The concentration of leptin (ng/mL) in the serum of mice was determined by ELISA. **b**, mRNA expression level s of SOCS-3, PTP1B and PI3K of arcuate nucleus in mice of pair-feeding assay. **c**, mRNA expression levels of c-FOS. *P* values were determined by a two-tailed Wilcoxon test, and data are presented as the means ± s.e.m*; P* < 0.05 (*); *P* < 0.01 (**); *P* < 0.001 (***).

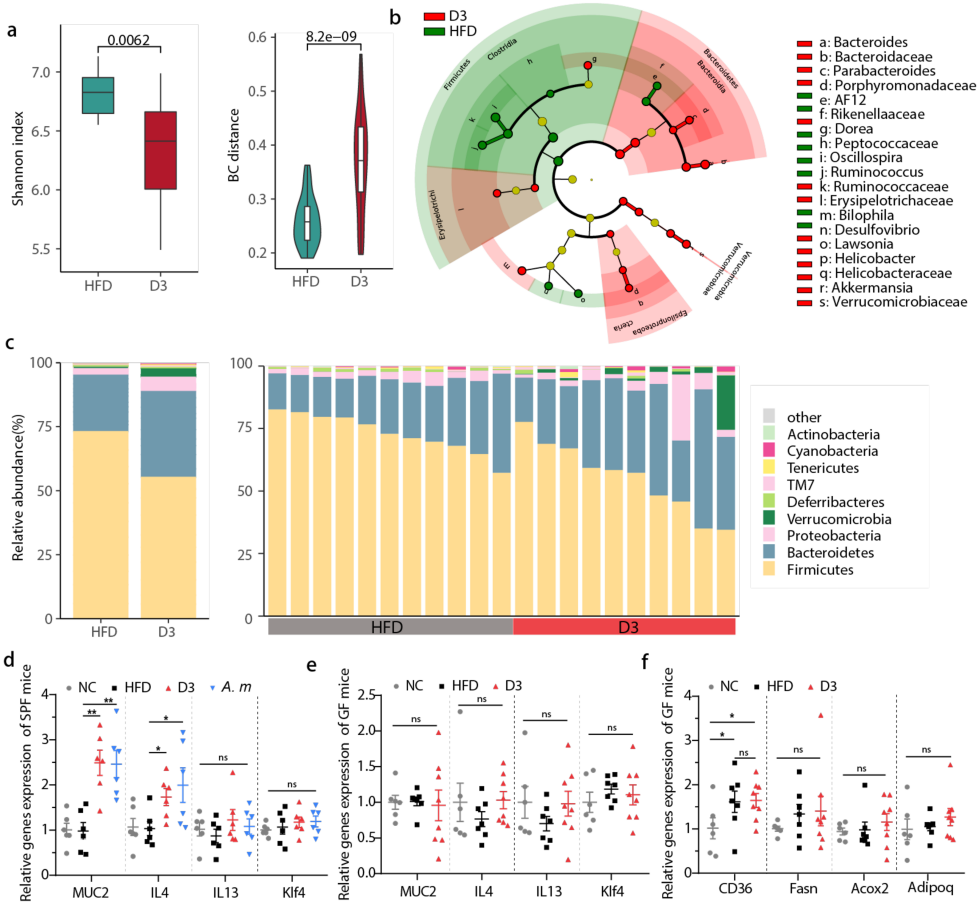

Supplementary Figure 5. Altered gut microbiota by D3 can affect gene expression in ileum of mice. a, Microbial diversity of the gut microbiota in mice, and the Bray-Curtis (BC) distance of the microbial communities between different groups. **b**, Cladogram representing significantly enriched taxa in D3 (red) or HFD (green). **c**, Fecal microbiota composition in HFD and D3 treated mice at a phylum level. The two bars on the left show the average relative abundance of each phylum. **d**, MUC2, IL4, IL13, and Klf4 mRNA expression levels in the colon of SPF mice fed on control diet (NC and HFD) or treated with D3 or gavaged with *A. muciniphila* (n = 6 mice per group). **e**, MUC2, IL4, IL13, and Klf4 mRNA expression levels in the colon of GF mice fed on control diet (NC and HFD) or treated with D3 (n = 6-8 mice per group). **f**, CD36, Fasn and Acox2 (liver) and Adipoq (epididymis) mRNA expression levels of GF mice fed on control diet (NC and HFD) or treated with D3 (n = 6 mice per group). *P* values were determined by two-tailed Wilcoxon test and data are presented as means ± s.e.m; *P* >0.05 (ns); *P* <0.05 (*); *P* <0.01 (**).

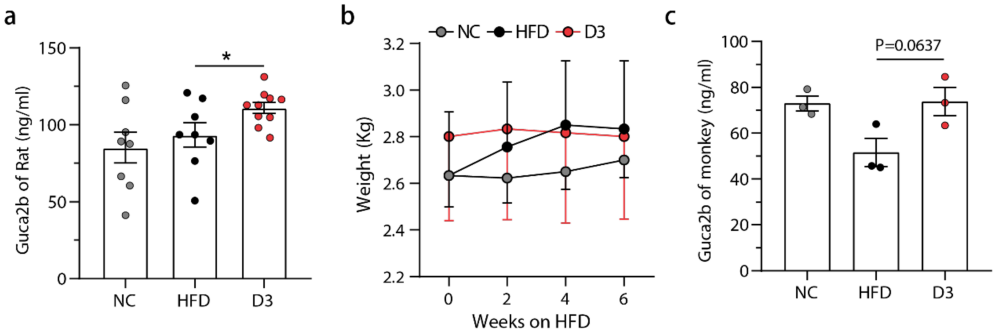

Supplementary Figure 6. Altered gut microbiota by D3 can affect gene expression in ileum of mice. a, The concentration of UGN (ng/mL) in the serum of rat was determined by ELISA. **b**, Kilograms of weight gain measured over time (n=3 macaques per group). **c**, The concentration of UGN (ng/mL) in the serum of macaques was determined by ELISA *P* values were determined by two-tailed Wilcoxon test and data are presented as means ± s.e.m; $P > 0.05$ (ns); $P < 0.05$ (*).

Supplementary Table 1. Physicochemical properties of peptides.

Peptide	HD5(1-9)	D1	D2	D3	D4
Charge	2	2	3	4	3
Prob of N-in[a]	0.91230	0.93899	0.93899	0.96573	0.95136

[a] Total prob of N-in: The total probability that the N-term is on the cytoplasmic side of the membrane.

Supplementary Table 2. The primers used in qPCR analysis.

Target	Primer	Sequence (5'-3')
Guca2b	Forward	GTACAGGCTGCTGATGAAATGAC
	Reverse	GGATGGCGATTACTTCAATGGTG
Leptin	Forward	TCTGAAAGATCCCACGTGCC
	Reverse	GGCTCAGGACATTCCAGCTT
CD36	Forward	GACGTGGCAAAGAACAGCAG
	Reverse	ATGGCTCCATTGGGCTGTAC
Fasn	Forward	AGCAGTATGTGACCACTGTGAG
	Reverse	TGATCCTCCTCTTCCAAGCAAC
Acox2	Forward	AGGCCATGTCTTCAGACTTCTG
	Reverse	CCTCATACGTGCAAGAGGCTAT
Adipoq	Forward	CCTGGCCACTTTCTCCTCATT
	Reverse	AAGAGGAACAGGAGAGCTTGC
Klf4	Forward	AGGAACTCTCTCACATGAAGC
	Reverse	CCTCTCTTGCTCAGTGTCCT
IL4	Forward	TGAGTCCAAGTCCACATCACTG
	Reverse	GGTCGTTGAACTCCTCGGTC
IL13	Forward	TCTCCCTCTGACCCTTAAGGAG
	Reverse	AGAGGCCATGCAATATCCTCTG
MUC2	Forward	AGGGCTCGGAACTCCAGAAA
	Reverse	CCAGGGAATCGGTAGACATCG
GAPDH	Forward	AACAGCAACTCCCACTCTTC
	Reverse	CCTCTCTTGCTCAGTGTCCT
Igrm1	Forward	CTTTCCCAATGTGGTGCTGTG
	Reverse	AACCTCTTTCCCATGCTCTGG
IFN-γ	Forward	CCACGGCACAGTCATTGAAAG
	Reverse	TGCTGATGGCCTGATTGTCTT
16S RNA	1369F	CGGTGAATACGTTCYCGG
	1492R	GGWTACCTTGTTACGACTT
A. muciniphila	Forward	CAGCACGTGAAGGTGGGGAC
	Reverse	CCTTGCGGTTGGCTTCAGAT

Cebpa-3	Forward	AGAACAGCAACGAGTACCGG
	Reverse	TGGTCAACTCCAGCACCTTC
C-FOS	Forward	TGGATTTGACTGGAGGTCTGC
	Reverse	CGTTGCTGATGCTCTTGACTG
AgRP	Forward	CTTCCACCTTTGCAGCATTCC
	Reverse	ACACGTGACTGCTTCCTGTAG
POMC	Forward	ATGCCGAGATTCTGCTACAGTC
	Reverse	CACCAGCTCCACACATCTATGG
PI3K	Forward	CTGAAGGCTATAAACGTGCAGC
	Reverse	CCTTTCTGGCATCCTGTACACT
PTP1B	Forward	CCCATCTTCCGTGGACATCAA
	Reverse	AGAGCTCCTTCCACTGATCCT
SOCS-3	Forward	ACTCTGACTCTACACTCGCCT
	Reverse	CGTGAAGTCTACAAAGGGGCT
NR2B	Forward	CCATGAACGAGACTGACCCAA
	Reverse	GAAATCGAGGATCTGGGCGAT
UCP-1	Forward	TGACTATGGTGCGCACAGAG
	Reverse	CTGCCACACCTCCAGTCATT
UCP-3	Forward	GATACATGAACGCTCCCCTAGG
	Reverse	GGCCCTCTTCAGTTGCTCATAT
Prdm16	Forward	AATGGACAAACGGCCTGAGAT
	Reverse	AATGGACAAACGGCCTGAGAT
CIDEA	Forward	GATGCACAAGCTTCAAGGCC
	Reverse	TGTATCGCCCAGTACTCGGA
Pgc1a	Forward	AGCCGTGACCACTGACAACGAG
	Reverse	AGCCGTGACCACTGACAACGAG
IL22	Forward	TCCCATCACAAGCAGAGACAC
	Reverse	TCCCATCACAAGCAGAGACAC
NR1D1	Forward	GGTGGTAGAGTTTGCCAAACAC
	Reverse	GGTGGTAGAGTTTGCCAAACAC
IL6	Forward	CTGCAAGAGACTTCCATCCAGT
	Reverse	CTGCAAGAGACTTCCATCCAGT
IL1β	Forward	AGGCTGACAGACCCCAAAAG
	Reverse	AGGCTGACAGACCCCAAAAG
TNF-α	Forward	CTGTGCCTCAGCCTCTTCTC
	Reverse	CTGTGCCTCAGCCTCTTCTC

1 Everard A, Lazarevic V, Derrien M, *et al.* Responses of Gut Microbiota and Glucose and Lipid Metabolism to Prebiotics in Genetic Obese and Diet-Induced Leptin-Resistant Mice. Diabetes

2011;**60**:2775-86.

2 Cheng YC, Liu JR. Effect of Lactobacillus rhamnosus GG on Energy Metabolism, Leptin Resistance, and Gut Microbiota in Mice with Diet-Induced Obesity. Nutrients 2020;**12**.

3 Folgueira C, Beiroa D, González-Rellán MJ*, et al.* Uroguanylin Improves Leptin Responsiveness in Diet-Induced Obese Mice. Nutrients 2019;**11**:752.

4 de Lartigue G, Barbier de la Serre C, Espero E*, et al.* Diet-induced obesity leads to the development of leptin resistance in vagal afferent neurons. American journal of physiology Endocrinology and metabolism 2011;**301**:E187-E95.

5 Kim GW, Lin JE, Snook AE*, et al.* Calorie-induced ER stress suppresses uroguanylin satiety signaling in diet-induced obesity. Nutr Diabetes 2016;**6**:e211.

6 Sato S, Basse AL, Schönke M*, et al.* Time of Exercise Specifies the Impact on Muscle Metabolic Pathways and Systemic Energy Homeostasis. Cell Metabolism 2019;**30**:92-110.e4.

7 Bibiloni R, Waget A, Neyrinck AM*, et al.* Changes in gut microbiota control metabolic endotoxemia-induced inflammation in high-fat diet-induced obesity and diabetes in mice.

8 Cani PD, Amar J, Iglesias MA*, et al.* Metabolic Endotoxemia Initiates Obesity and Insulin Resistance. Diabetes 2007;**56**:1761.

9 Everard A, Belzer C, Geurts L*, et al.* Cross-talk between Akkermansia muciniphila and intestinal epithelium controls diet-induced obesity. Proc Natl Acad Sci U S A 2013;**110**:9066-71.

10 Pertea M, Kim D, Pertea GM*, et al.* Transcript-level expression analysis of RNA-seq experiments with HISAT, StringTie and Ballgown. Nature protocols 2016;**11**:1650.

11 Walter W, Sánchez-Cabo F, Ricote M. GOplot: an R package for visually combining expression data with functional analysis. Bioinformatics 2015;**31**:2912-4.